Charmonium in strongly coupled quark-gluon plasma

Clint Young and Edward Shuryak
Department of Physics and Astronomy, State University of New York, Stony Brook, New York 11794-3800, USA
(Received 22 September 2008; revised manuscript received 14 January 2009; published 19 March 2009)

The growing consensus that a strongly coupled quark-gluon plasma (sQGP) has been observed at the SPS and RHIC experiments suggests a different framework for examining heavy-quark dynamics. We present both a semianalytical treatment of Fokker-Planck (FP) evolution in pedagogical examples and numerical Langevin simulations of evolving $c\bar{c}$ pairs on top of a hydrodynamically expanding fireball. In this way, we may conclude that the survival probability of bound charmonia states is greater than previously estimated, as the spatial equilibration of pairs proceeds through a "slowly dissolving lump" stage related to the pair interaction.

DOI: 10.1103/PhysRevC.79.034907 PACS number(s): 25.75.Cj

I. INTRODUCTION

A. Overview

Charmonium suppression is one of the classical probes used in heavy-ion collisions. Since charm quark pairs originate during early hard processes, they go through all stages of the evolution of the system. A small fraction of such pairs [$\sim O(10^{-2})$] produces bound $\bar{c}c$ states. By comparing the yield of these states in AA collisions to that in pp collisions (where matter is absent) one can observe their survival probability, giving us important information about the properties of the medium.

Many mechanisms of J/ψ suppression in matter were proposed over the years. The first, suggested by one of us in 1978 [1], is (i) a gluonic analog to the "photoeffect" $gJ/\psi \to \bar{c}c$. Perturbative calculations of its rate [2] predict a rather large excitation rate of the charmonium ground state. Since charmonia are surrounded by many gluons in (QGP), this led to a conclusion by Kharzeev and Satz [2] that nearly all charmonium states at RHIC should be rapidly destroyed. If so, the observed J/ψ would come mostly from recombined charm quarks at chemical freezout, as advocated in Ref. [3].

However, this argument is only valid in weakly coupled QGP, in which the charm quarks would fly away from each other as soon as enough energy is available. As we will show in the following, in strongly coupled QGP (sQGP) the propagation of charmed quarks is in fact very different. Multiple momentum exchanges with matter will lead to rapid equilibration in momentum space, whereas motion in position space is slow and diffusive in nature. Persistent attraction between quarks makes the possibility of returning back to the ground state for the J/ψ quite substantial, leading to a substantial survival probability even after several fm/c time in sQGP.

Another idea (ii) proposed by Matsui and Satz [4] focuses on the question of whether charmonium states do or do not survive *as a bound state*. They argued that because of the deconfinement and the Debye screening, the effective $\bar{c}c$ attraction in QGP is simply too small to hold them together as bound states. Quantum-mechanical calculations by Karsch *et al.* [5] and others have used the free energy, obtained from the lattice, as an effective potential (at $T > T_c$):

$$F(T,r) \approx -\frac{4\alpha(s)}{3r}\exp[-M_D(T)r] + F(T,\infty). \qquad (1)$$

They have argued that as the Debye screening radius M_D^{-1} decreases with T and becomes smaller than the root-mean-square radii of corresponding states $\chi, \psi', J/\psi, \Upsilon'', \Upsilon', \Upsilon, \ldots$, those states should subsequently melt. Furthermore, it was found that for J/ψ the melting point is nearly exactly T_c, making it a famous "QGP signal."

These arguments are correct asymptotically at high enough T, but the central issue is what happens at (so far experimentally accessible at RHIC) $T = (1\text{–}2)T_c$. Dedicated lattice studies [6] extracted quarkonia spectral densities using the so-called maximal entropy method (MEM) to analyze the temporal (Euclidean time) correlators. In contrast to the aforementioned predictions, the peaks corresponding to η_c, J/ψ states remain basically unchanged with T in this region, indicating the dissolution temperature is as high as $T_\psi \approx (2.5\text{–}3)T_c$. Mocsy *et al.* [7] have used the Schrödinger equation for the Green function to find an effective potential that would describe best not only the lowest s-wave states but the whole spectral density. Recently [8], they have argued that a near-threshold enhancement is hard to distinguish from a true bound state: According to these authors, the MEM dissolution temperature is perhaps too high.

Another approach to charmonium in heavy-ion collisions, taken by Grandchamp and Rapp [9], describes how charmonium states can continue to be observed in heavy-ion collisions for a different reason. This model still has fairly large cross sections for J/ψ annihilation, so in their so-called two-component model, many of the final charmonia measured are required to originate from statistical coalescence of single charm in the plasma into charmonium states, both of "diagonal" charm pairs originating from the same high-energy initial event and of "nondiagonal" pairs originating from different events.

There are also other quantum-mechanical studies of the issue since the pioneering paper of Karsch *et al.* [5]. Shuryak and Zahed [10] argued that one should not use the free energy $F(T,r)$ as the effective potential, because it corresponds to

a static situation in which infinite time is available for a "heat exchange" with the medium. In the dynamical real-time situation they proposed to think in terms of level crossing and Landau-Zener formalism, widely used in various quantum-mechanical applications. In the "fast" limit (opposite to the "adiabatically slow" one) all level crossings should instead be ignored. This corresponds to retaining pure states (described by a wave function rather than density matrix) without the *entropy term* in F, which is nothing else but the internal energy

$$V(T,r) = F(T,r) - TdF(T,r)/dT = F + TS \qquad (2)$$

instead, as an alternative effective potential. Such a potential $V(T,r)$ (extracted from the same lattice data) leads to much more stable bound states, putting charmonium melting temperature to higher $T \sim 3T_c$. A number of authors [11] have used effective potentials in between those two limiting cases. However, as will become clear from what follows, we think it is not the bound states themselves that are important, but the kinetics of transitions between them. In a nutshell, the main issue is *how close to each other are $\bar{c}c$ states when the QGP is over*, not in which particular states they have been during this time.

The heavy $Q\bar{Q}$ potential depends not only on the temperature but also on the velocity of the $\bar{c}c$ pair relative to the medium. This effect has been studied, for example, by means of the anti-de-Sitter space/conformal field theory (AdS/CFT) correspondence in Ref. [12] and it was found that the bound state should not exist above a certain critical velocity. So, if the existence of a bound state is truly a prerequisite for J/ψ survival, one would expect additional suppression at large p_t. This goes contrary to the well-known formation-time argument [13] and the experimental evidence, indicating the disappearance of the J/ψ suppression at large p_t. We think this as a good example of the importance of the real-time dynamics of the $\bar{c}c$ pair in medium and indeed we are going to follow it in the following from its birth to its ultimate fate.

Let us now briefly review the experimental situation. For a long time it was dominated by the SPS experiments NA38/50/60, in which observations were made of both "normal" nuclear absorption and an "anomalous" suppression, maximal in central Pb + Pb collisions. Since at RHIC QGP has a longer lifetime and reaches a higher energy density, straightforward extrapolations of the naive J/ψ melting scenarios predicted near-total suppression. And yet, the first RHIC data apparently indicate a survival probability similar to that observed at the SPS.

One possible explanation [14] is that the J/ψ suppression is canceled by a recombination process from unrelated (or nondiagonal) $\bar{c}c$ pairs floating in the medium. However, this scenario needs quite accurate fine-tuning of two mechanisms. It also would require rapidity and momentum distributions of the J/ψ at RHIC to be completely different from those in a single hard production.

Another logical possibility [15] is that the J/ψ actually does survive both at SPS and RHIC; the anomalous suppression observed may simply be due to suppression of higher charmonium states, ψ' and χ, feeding down about 40% of J/ψ in pp collisions. These authors however have not attempted to explain why the J/ψ survival probability can be close to one.

This is precisely the goal of the present work, in which we study dynamically *how* survival of J/ψ happens. We will see that it is enhanced by two famous signatures of sQGP, namely (i) a *very small charm diffusion constant* and (ii) a *strong mutual attraction* between charmed quarks in the QGP. We found that J/ψ survival through the duration of the QGP phase ($\tau \sim 5$ fm/c) is about a half.

The sequence of events can be schematically described as a four-stage process:

$$\frac{\Longrightarrow}{(\bar{c}c \text{ production})} f_{\text{initial}} \frac{\Longrightarrow}{(\text{momentum relaxation})} f_{\text{quasiequilibrium}} \times \frac{\Longrightarrow}{(\text{leakage})} f_{\text{final}} \frac{\Longrightarrow}{(\text{projection})} J/\psi. \qquad (3)$$

A new element here is a two-time-scale evolution, including rather rapid momentum relaxation to a quasiequilibrium distribution, which differs from the equilibrium one at large enough distances.

B. Charmonium potentials at $T > T_c$

The interaction of the $\bar{c}c$ pairs will play a significant role in this paper, and thus we briefly review what is known about them. The details can be found in the original lattice results. We will point out only the most important qualitative features.

Perturbatively, at high T one expects a Coulomb-like force, attractive in the color singlet and repulsive in the color octet channel, with the relative strengths 8:(−1) (so that color average will produce zero effect). As shown by one of us many years ago [1], the Coulomb forces are screened by the gluon polarization operator at distances $\sim 1/gT$.

Quantitative knowledge of the interaction comes from a large set of lattice measurements of the free energies associated with a pair of heavy quarks in an equilibrium heat bath. These data include both results by the Bielefeld-BNL group and in dynamical QCD with $N_f = 2$ by Aarts *et al.* [16].

At $T > T_c$ one has a deconfined phase, so at large quark separations one expects effective potentials to go to a *finite* $V_\infty(T)$. Yet when the value of this potential significantly exceeds the temperature, the actual probability of quark separation is small ($\sim \exp[-V_\infty(T)/T]$). As we already mentioned in the preceding section, the appropriate potential for a dynamical $\bar{c}c$ pair is not yet definitely determined, with suggestions ranging from free energy to potential energy measured on the lattice.

The difference between the two—the entropy associated with the $\bar{c}c$ pair—is very large near T_c, reaching the value $S \sim 20$ at its peak. It means that a huge number of excited states [$\sim \exp(S) \sim \exp(20)$] would be excited in adiabatically slow motion of the pair. We think that in realistic $\bar{c}c$ pair motion considerably fewer states are actually excited, and thus, following Ref. [10], we will use the potential energy instead of free energy. The cost of this is a much larger potential barrier, reducing $\bar{c}c$ dissociation. Indeed, $V_\infty(T)$ near T_c is large, reaching about 4 GeV at its peak.

For the simulation we need a parametrization of the heavy quark-antiquark potential above deconfinement as a function of temperature and separation. We use the same

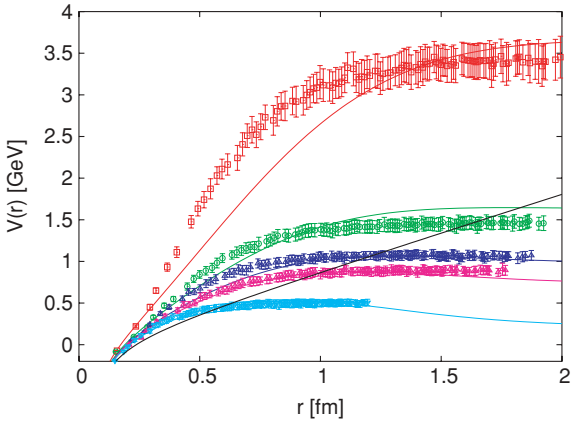

FIG. 1. (Color online) Parametrization of the potential for lattice data from Ref. [17]. From top to bottom are the potentials at $T/T_c =$ 1.02, 1.07, 1.13, 1.18, and 1.64.

parametrization as in Ref. [7]:

$$V(r,T) = -\alpha\frac{e^{-\mu(T)r^2}}{r} + \sigma r e^{-\mu(T)r^2} + C(T)\left(1 - e^{-\mu(T)r^2}\right) \tag{4}$$

and fit to quenched-QCD lattice data in a temperature range of $1.02T_c$ to $1.64T_c$, assuming σ is constant in temperature, μ varies linearly with temperature over this range, and $C(T) \propto (T/T_c - 0.98)^{-1}$, so that it peaks sharply at T_c as $U_{\rm inf}$ does. The result shown in Fig. 1 is for

$$\mu(T) = (0.03 + 0.006T/T_c)\ \text{GeV}^2, \tag{5}$$

$$\sigma = 0.22\ \text{GeV}^2, \tag{6}$$

and

$$C(T) = \frac{0.15\ \text{GeV}}{T/T_c - 0.98}, \tag{7}$$

with α set to $\frac{\pi}{12}$.

As you can see from Fig. 1, this fit is not perfect. Although it is easy to fit a function to a single temperature's data set, it is hard to find an adequate fit across temperatures. This fit however will prove sufficient, especially since it is relatively good for the small separations of interest.

The classical Boltzmann factor $\exp[U(r)/T]$ for a Coulomb potential leads to a non-normalizable distribution. Quantum mechanics prevents this, which can be crudely modeled by an effective potential

$$V_{\rm eff} = \hbar^2/Mr^2 + V(T,r), \tag{8}$$

which includes the so-called localization energy. Dusling and one of us [18] have determined more accurate effective quantum potentials, following the ideas of Kelbg and others and performing path integrals. Perhaps those should be used in future more sophisticated simulations. In the present simulations we simply turn off the force below 0.2 fm, approximating the effective potential by a constant.

During the simulation, we allow our pairs to exist as either color singlets or color octets. Whereas in a zero-temperature pp collision, confinement completely suppresses a $\bar{c}c$ pair's probability of existing in a color octet state, in the deconfined phase this possibility must be considered. We initially create a 1:8 ratio of color singlet to color octet pairs, as is expected statistically, and then during each time step we decide if the pair exists as a color octet by comparing a random number between zero and one to $\frac{1}{Z}\exp[-(U_8 - U_1)/T)]$, with the color singlet and octet potential energies determined from Ref. [19]. In other words, the pairs exist in thermal equilibrium in color space at all times. When a pair exists as a color octet, it do not interact in our simulation as the spatial variation of the octet free energies is quite small.

Naively, one would expect this to create a large difference with results where color singlet states are assumed for all pairs; however, this is not the case. One sees this by noticing that for the temperatures and distances of our interest (distances of separation for pairs likely to go into the J/ψ state), $\frac{U_8 - U_1}{T} \sim 10$, meaning that the octet state is suppressed by orders of magnitude.

Lattice potentials do not follow simple perturbative relations. The potential $V_1 = -8V_8$ between singlet and octet potentials previously mentioned does not hold nonperturbatively [19]. Whereas the color singlet channel displays a significant attraction, the color octet channel has a potential that is remarkably flat (r-independent). On the basis of this feature of the lattice data we will ignore the force in the octet channel in the simulation.

C. Charm diffusion constant

Loosely speaking, the effect we are after in this work can be expressed as follows: The medium is trying to prevent the outgoing quarks from being separated. It has been conjectured by one of us that charm quark pairs should get stopped in QGP [20]. RHIC single electron data suggest that charm quarks, and probably bottom quarks as well, are indeed equilibrating much more effectively than was previously thought [21].

The first question one should address is how a charm-anticharm pair moves in sQGP and the probability of finding the $\bar{c}c$ in close proximity after time t. Charm quarks are subject to three forces: the drag force, the stochastic force from a heat bath, and the $\bar{c}c$ mutual interaction.

(i) The drag force tries to reduce the difference between the quark momentum distribution and that in the (local) equilibrium quark and matter velocities.
(ii) The stochastic (or Langevin) force from a heat bath leads to thermal equilibration in momenta and spatial diffusion of the charm quarks.
(iii) For pedagogical reasons it is useful to include the $\bar{c}c$ mutual interaction, first for stationary nonfloating matter at fixed temperature (using the Fokker-Planck equation) and then for a realistic nuclear geometry with a hydrodynamically expanding fireball.

Before we proceed, let us briefly recall why the case of heavy (charmed) quarks is so special. (A more detailed discussion of the subject can be found in Moore and Teaney [22].) A collision of a heavy quark with the quasiparticles of QGP leads to a change in its momentum $\Delta p_{\rm HQ} \sim T$, so that

the velocity is changed by a small amount

$$\Delta v_{\rm HQ} \sim T/M_{\rm HQ} \ll 1. \tag{9}$$

Therefore the velocity of the charm quark can only change significantly as a result of multiple collisions, in small steps. Thus the process can be described via appropriate differential equations such as the Fokker-Planck or the Langevin equations. Similarly, one can argue that spatial diffusion of a heavy particle can also be described in this way, because the changes in position between collisions are small and uncorrelated.

An assumption necessary for Langevin dynamics to hold is that the "kicks" are random (uncorrelated). As just explained, for a single heavy quark, this follows from the inequality $M \gg T$, which guarantees that the quark relaxation time is long compared to the correlation time in matter. For a $\bar{c}c$ pair we need an additional requirement, that random forces on each quark can be treated as *mutually* uncorrelated. To see how good this approximation is, one should compare the spatial (equal-time) correlation length $\xi(T)$ in the medium to the typical distance between quarks for paths that eventually (at the end of the plasma era) will become charmonia. We will provide two different estimates for the former quantity, which view QGP either as a perturbative "gas" or a strongly coupled "liquid."

In a perturbative gas of gluons, the mass is small and in the lowest order the momentum distribution is thermal. Thus the maximum of the momentum distribution is at $p \approx 2.7T$, about 1 GeV at the initial RHIC condition. The corresponding half-wavelength (the region where the field keeps at least its sign) is

$$\lambda/2 = \pi/p \approx 0.6\ {\rm fm} \sim \xi(T = 0.4\ {\rm GeV}). \tag{10}$$

In the liquid regime quasiparticles do not successfully model the degrees of freedom. However, we do have phenomenological information about spatial correlations from hydrodynamics, in which the so-called sound absorption length can be proposed as a measure above which different matter "cells" decorrelate. It is

$$\Gamma_s = \frac{4\eta}{3sT}, \tag{11}$$

with η/s as the dimensionless ratio of viscosity to entropy density. Empirically, RHIC data are well described if this ratio is of the order of $1/3\pi$ (the AdS/CFT strong-coupling limit), which suggests a spatial correlation length one order of magnitude smaller [$\xi(T = 0.4\ {\rm GeV}) \sim 0.05$ fm].

Since the distance between the $\bar{c}$ and the c that eventually become J/ψ is about 0.5 fm, and since there are good reasons to believe the latter "liquid" estimate of ξ is closer to reality, we conclude that the main Langevin assumption—the independence of random forces for $\bar{c}$ and c—is well justified. Furthermore, one may think that the same assumption would even hold for $\bar{b}$ and b, although with poorer accuracy.

Since this small parameter in Eq. (9) is central to what follows, let us recall that at RHIC we speak about the ratio for the charmed quark of $T/M_c = (1/6–1/5)$, or $T/M_b = (1/20–1/15)$ for the b quark.

Although RHIC experiments with charm quarks include direct reconstruction of the charmed mesons D and D^* by the STAR Collaboration, so far the existing vertex detectors are insufficient for doing this effectively (but upgrades are coming). Therefore the most relevant data on charm are based on observations of single electrons from heavy-quark weak semileptonic decays. Apart from electromagnetic backgrounds, we do not really know whether electrons come from c or b decays: It is believed (but not yet proven) that the boundary between two regimes is at $p_t \approx 4$ GeV. Two experimentally observable quantities are (i) the charm suppression relative to the parton model (no matter) R^e_{AA} and (ii) the azimuthal asymmetry of the electrons relative to the impact parameter $v^e_2 = \langle \cos(2\phi) \rangle$.

Several theoretical groups have analyzed these data, in particular Moore and Teaney [22] provided information about the diffusion constant of a charm quark D_c by Langevin simulations. A conclusion following from this work is that both R^e_{AA} and v^e_2 observed at RHIC can be described by one value for the charm diffusion constant in the range

$$D_c\ (2\pi T) = 1.5–3. \tag{12}$$

This can be compared with the perturbative (collisional) result at small α_s of

$$D_c^{\rm pQCD}\ (2\pi T) = 1.5/\alpha_s^2. \tag{13}$$

Assuming that the perturbative domain starts[1] somewhere at $\alpha_s < 1/3$ one concludes that the empirical value [Eq. (12)] is an order of magnitude smaller than the perturbative value.

There are two studies of the diffusion constant at strong coupling. One comes from AdS/CFT correspondence [23] (and thus the results are for $\mathcal{N} = 4$ supersymmetric Yang-Mills theory). The final expression found by Casalderrey-Solana and Teaney [24] is

$$D_{\rm HQ} = \frac{2}{\pi T \sqrt{g^2 N_c}}. \tag{14}$$

It is nicely consistent (via the Einstein relation) with the calculated drag force

$$\frac{dP}{dt} = -\frac{\pi T^2 \sqrt{g^2 N_c} v}{2\sqrt{1 - v^2}} \tag{15}$$

by Herzog *et al.* [25]. One assumption of this calculation is that the 't Hooft coupling is large ($g^2 N_c \gg 1$), which means the diffusion constant is parametrically small, being much less than momentum diffusion in the same theory [$D_p = \eta/(\epsilon + p) \sim 1/4\pi T$]. This result is also valid only for quarks with masses

$$M_{\rm HQ} > M_{\rm eff} \sim \sqrt{g^2 N_c} T, \tag{16}$$

which only marginally holds for charm quarks.

Let us see what these numbers mean for RHIC (assuming that they are valid for QCD). The 't Hooft coupling $g^2 N_c = \alpha_s 4\pi N_c \approx 20–40$ is indeed large, but $M_{\rm eff} \approx 1–2$ GeV is not really small as compared to the charm quark mass; thus the derivation is only marginally true. Yet we proceed and get

$$D_c\ (2\pi T) = 4/\sqrt{g^2 N_c} \sim 0.5–1, \tag{17}$$

[1]Recall that at $4/3\alpha_s = 1/2$ two scalar quarks should fall toward each other, according to the Klein-Gordon equation, so this is clearly not a perturbative region.

which is in within the right ballpark of phenomenological numbers.

Another approach to transport properties of strongly coupled plasmas involves classical molecular dynamics. A classical non-Abelian model for sQGP was suggested by Gelman *et al.* [26], and recently Liao and Shuryak [27] have added magnetically charged quasiparticles. Those calculations also reveal that the diffusion constant D rapidly decreases as a function of the dimensionless coupling constant Γ as a power:

$$D \sim \left(\frac{1}{\Gamma}\right)^{0.6-0.8}, \tag{18}$$

where in a liquid domain $\Gamma = 1$–100. Qualitatively, it is similar to $1/\sqrt{g^2 N_c}$ of the AdS/CFT result [Eq. (17)]. Unfortunately, at this moment there is no deep understanding of the underlying mechanism of both strong coupling calculations.

However, this subject is well beyond the aims of the present work. In what follows we will use $D_c\,(2\pi T) = 1.5$–3 as a range for our best current guess.

II. CHARMONIUM IN sQGP: FOKKER-PLANCK FORMALISM

Before we describe realistic Langevin simulations of RHIC collisions it is useful to see first the basic features analytically. In this section we start with a pedagogical example of very high drag, whose influence can be separated from that of diffusion. So, instead of the Fokker-Planck equation, a partial differential equation in six dimensions will be solved numerically in the following. We will start with ordinary differential equations including the effect of drag only. We describe how the high drag coefficient η_c causes rapid thermalization of the initially hard momentum distribution from the particle physics event generator PYTHIA and how the small diffusion coefficient D_c, inversely proportional to η_c, combined with the use of the static $Q\bar{Q}$ internal energy instead of the free energy for the pair interaction leads to a slow dissolution of a large peak in the distribution in position space, causing less suppression than expected by more naive models.

To see the first feature, rapid thermalization in momentum space, consider a $\bar{c}c$ pair with the quarks emerging back to back from a hard process with momentum $\mathbf{p} \gg T$ and therefore having relative momentum $\Delta\mathbf{p} = 2\mathbf{p}$. For $\mathbf{p} \gg T$, as is the case initially for charm quarks created at the RHIC, we may neglect the random kicks that the quarks experience from the medium and consider only the drag: $\frac{d(\Delta\mathbf{p})}{d\tau} = -\eta_c \mathbf{p}$, where $\eta_c = \frac{T}{M_c D_c}$. This leads to a very simple formula for the relative momentum of a pair at early times:

$$\Delta\mathbf{p}(t) = \exp(-\eta_c \tau)\Delta\mathbf{p}(0). \tag{19}$$

Using the AdS/CFT value for the diffusion coefficient, this leads to a drag coefficient $\eta_c \approx 0.6$ GeV.

Let us now examine the distribution of $\bar{c}c$ pairs created with PYTHIA pp-event generation at energies of 200 GeV. (See further discussion of this in Sec. III.) The initial transverse momentum distribution[2] is broad compared to the thermal distribution, and therefore we may apply Eq. (19) for early times. We parametrize the initial relative momentum distribution as in Sec. III B and replace $\Delta\mathbf{p}$ with $\Delta\mathbf{p}\exp(\eta_c\tau)$, which is the formula for a pair's *initial* relative momentum in terms of its relative momentum at proper time τ. Next, we compute the overlap of this distribution at early times with the J/ψ state's Wigner quasiprobability distribution to determine the probability of a random $\bar{c}c$ taken from this ensemble to be measured as a J/ψ particle, an approach detailed in Appendix B.

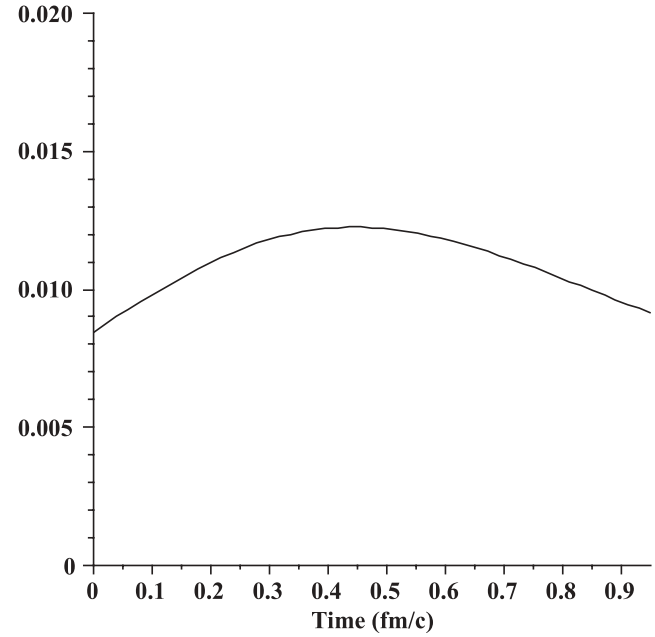

FIG. 2. Probability of a $\bar{c}c$ pair going into the J/ψ state vs time, for very early time.

Figure 2 shows this probability as a function of time for $\eta_D = 0.88$. The initial value of the projection is 0.8%, on the same order of magnitude as the experimental value of 1% for $\frac{\sigma_{J/\psi}}{\sigma_{c\bar{c}}}$ obtained from Refs. [28,29]. The projection increases as the PYTHIA-with-drag distribution narrows but then drops when the width shrinks more than the J/ψ's width in momentum space and as the quark pair's separation increases. Once the time reaches about 1 fm/c, the probability for a pair to go into a J/ψ state is about where we started, and we quit looking at this approach after this much time because the mean transverse momentum for a quark is the thermal average.

After this first 1 fm/c of the QGP phase, the $\bar{c}c$ distribution has thermalized in momentum space and the evolution in position space (diffusion) needs to be examined. The root-mean-square distance for diffusive motion is given by the

[2]The initial *rapidity* distribution is wide also, but since longitudinally Bjorken-like hydrodynamics starts immediately, a charm quark finds itself with comoving matter with the same rapidity, and thus it has little longitudinal drag. Transverse flow is slow to be developed, and thus there is transverse drag.

standard expression

$$\langle x^2 \rangle = 6 D_c \tau, \tag{20}$$

where τ is the proper time and the interaction between the quarks has been neglected. The "correlation volume" in which one finds a quark after time τ is

$$V_{\rm corr} = \frac{4\pi}{3}(6 D_c \tau)^{3/2}, \tag{21}$$

and one may estimate for the probability of the $\bar{c}c$ pair to be measured in the J/ψ state as

$$P(\tau) \sim R^3_{J/\psi}/(6 D_c \tau)^{3/2}. \tag{22}$$

So neglecting the pair's interaction leads to a small probability that J/ψ states will survive by the hadronization time at the RHIC ($\tau \sim 10$ fm/c), even for small values of the diffusion coefficient.

To get an idea for how this simple result is changed by the inclusion of an interaction between the constituent quarks in a given $\bar{c}c$ pair, let us examine the Fokker-Planck equation for the $\bar{c}c$ distribution in relative position:

$$\frac{\partial P}{\partial t} = D \frac{\partial}{\partial \mathbf{r}} f_0 \frac{\partial}{\partial \mathbf{r}} (P/f_0), \tag{23}$$

where $f_0(r) \propto \exp[-V_{\rm eff}(r)/T]$ is the *equilibrium* distribution in the magnitude of relative position r. By substituting the potential shown above at $T = 1.25 Tc$ and $D_c \times (2\pi T) = 1$ into the Fokker-Planck equation (for demonstration in a single spatial dimension only) we can solve it numerically and find how the relaxation process proceeds. A sample of such calculations is shown in Fig. 3. It displays two important features of the relaxation process:

(i) During a quite short time $T \sim 1$ fm/c, the initial distribution (peaked at zero distance) relaxes locally to the near-equilibrium distribution with two peaks, corresponding to optimal distances of the equilibrium distribution f_0, where the effective potential is most attractive.

(ii) The second stage displays a slow "leakage," during which the maximum is decreasing while the tail of the distribution at large distances grows. It is slow because the right-hand side of the Fokker-Planck equation is close to zero, as the distribution is nearly f_0. The interaction drastically changes the evolution of the $\bar{c}c$ distribution in position space, and this will be demonstrated again in the full numerical simulation of the next section.

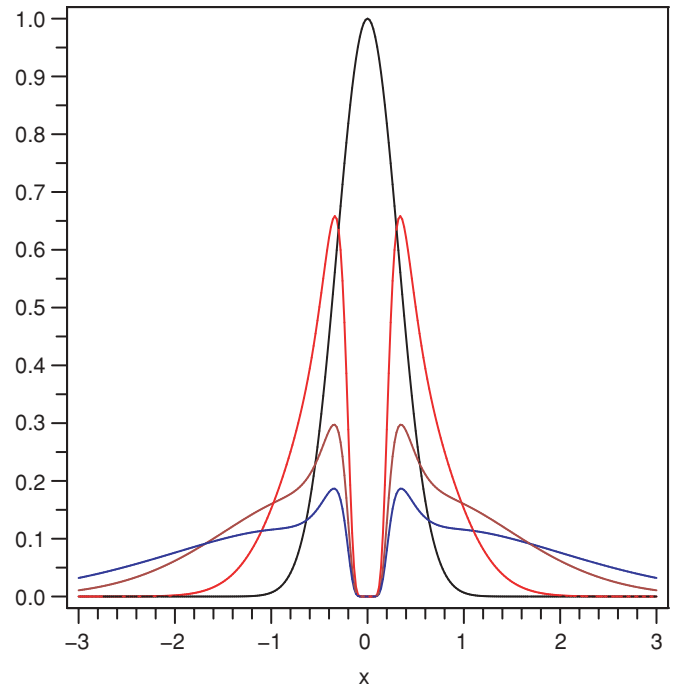

FIG. 3. (Color online) Numerical solution of the one-dimensional Fokker-Planck equation for an interacting $\bar{c}c$ pair. The relaxation of the initial narrow Gaussian distribution is shown by curves (in black, red, brown, green, and blue, from top to bottom at $r = 0$) corresponding to times $t = 0$, 1, 5, and 10 fm, respectively.

III. LANGEVIN EVOLUTION OF THE $\bar{c}c$ PAIRS

A. Langevin evolution in a static medium: quasiequilibrium

Before we turn our attention to the expanding fireball, we first study the evolution of $\bar{c}c$ pairs at various fixed temperatures above deconfinement and in the absence of hydrodynamical flows. The first thing we would like to demonstrate is the strong influence of the heavy-quark interaction. The resulting distributions over interquark separation at time 10 fm/c are shown in Fig. 4 with the interaction (red squares) and without (blue triangles). The value for a given pair's separation r is weighted by $\frac{1}{r^2}$ so that the spatial phase space of the distribution is divided out. With the interaction on, we find the same behavior of a "slowly dissolving lump" as that seen in the solution of the Fokker-Planck equation when the interaction is "turned on."

Further study of this has shown convergence to a particular shape, which persists for a long time and which we would

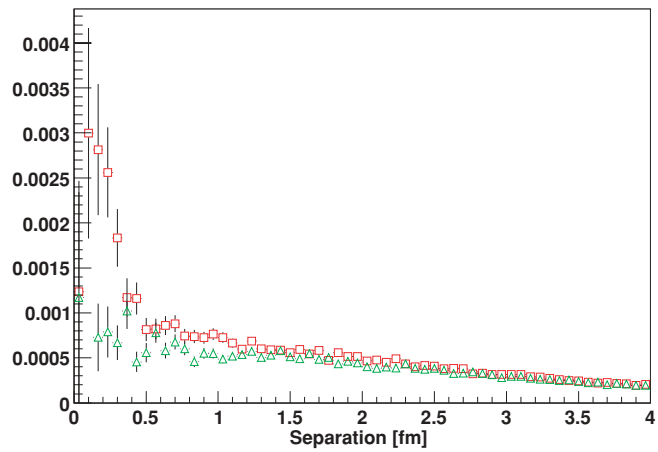

FIG. 4. (Color online) Distribution over quark pair separation at fixed $T = 1.5 T_c$ after 9 fm/c, with (red squares) and without (green triangles) the $\bar{c}c$ potential.

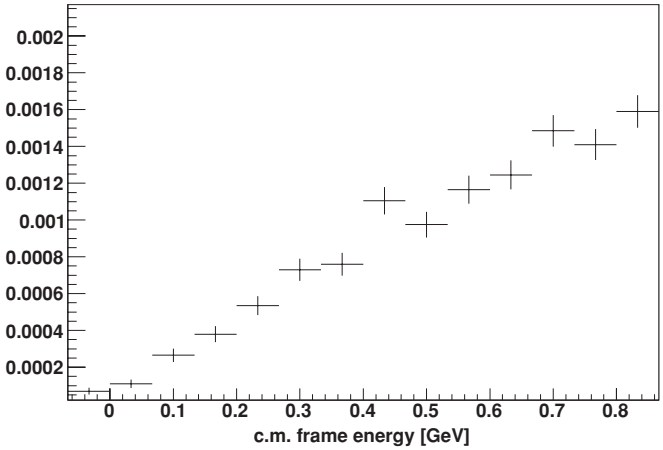

FIG. 5. Energy distribution of the $c\bar{c}$ pairs (in the center-of-mass frame of the pair) after Langevin evolution at a fixed temperature $T = 1.05T_c$ for a time $t = 9$ fm/c long enough for quasiequilibrium to be reached.

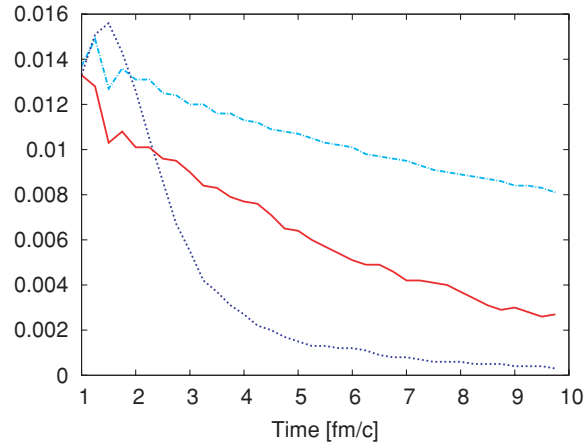

FIG. 6. (Color online) The probability for a $c\bar{c}$ pair to be bound, where $T = 1.1T_c$ is held fixed. The dotted (blue) curve shows a simulation without a pair interaction and $2\pi T D_c = 1.5$, the solid (red) curve shows $2\pi T D_c = 1.5$ with pair interaction, and the dot-dashed (green) curve shows $2\pi T D_c = 3.0$ with interaction.

call "quasiequilibrium."[3] Although the true equilibrium of course corresponds to complete dissolution of a single $\bar{c}c$ pair, it turns out that leakage to large distances affects the distributions of separation and energy in normalization only. Figure 5 shows the energy distribution for the ensemble of pairs at $\tau = 9$ fm/c after evolving under Langevin dynamics at a fixed temperature $1.05T_c$; it is shown to be the same distribution, up to normalization and statistical uncertainty, as the distribution reached by the pairs in a full heavy-ion simulation of the most central collisions.

We show the energy distribution in this region because it is related to a very important issue of the charmonium production, namely production of ψ', χ states and subsequent *feeddown* into the J/ψ. When a quasiequilibrium distribution is reached, the production ratios of charmonium states are stabilized at thermal (statistical) model values, in spite of the fact that the overall normalization continues to shrink owing to leakage into infinitely large phase space at large distances.

(The energy distribution itself contains a Boltzmann factor but also the density of states. A model case of a purely Coulomb interaction allows one to calculate it in a simple way. As shown in Appendix A we found that in this case the absolute shape of the quasiequilibrium distribution is reproduced as well.)

The existence of quasiequilibrium corresponds well to observations. It was noticed already a decade ago [30] that the SPS data on the centrality dependence of the $N_{\psi'}/N_{J/\psi}$ ratio approached the equilibrium value (for chemical freezout)

$$\frac{N_{\psi'}}{N_{J/\psi}} = \exp(-\Delta M/T_{\rm ch}) \tag{24}$$

with the chemical freezout at $T_{\rm ch} = 170$ MeV, as is observed for ratios of other hadronic species.

[3]This situation should not be confused with stationary nonequilibrium solutions of the Fokker-Planck equation, in which there is a constant flow through the distribution because of matching source and sink.

One possible explanation for this can be charmonium *recombination* (from independent charm quarks) at chemical freezout, advocated by Andronic *et al.* [3] and others. However, our findings show that the same ratio naturally appears even for a *single* $\bar{c}c$ pair dissolving in a thermal medium, in a "quasiequilibrium" occurring at the leakage stage. Especially at SPS, when statistical recombination requires a charm density that is too large, this is an attractive possibility.

At this point, it is interesting to start discussing what percentage of the charm pairs in our ensemble can be described as "bound." How we determine whether or not a pair is bound is discussed in Appendix B. Figure 6 shows how the percentage of charm pairs that are bound changes with proper time in a Langevin simulation where the temperature is held fixed at $T = 1.1T_c$. These simulations show how the charm pairs dissolve slowly and is affected by the interaction of the charm and anticharm quarks.

B. Production of the initial $\bar{c}c$ pairs

We start with $\bar{c}c$ events produced with PYTHIA, a particle physics event generator [31]. PYTHIA yields $\bar{c}c$ pairs through a set of perturbative QCD (pQCD) events: Through Monte Carlo simulation it will select initial partons from the parton distribution function of one's choosing and proceed through leading-order QCD differential cross sections to a random final state. The p_t and rapidity distributions of charm produced in pp collisions is believed to be adequately represented.

By using PYTHIA we do not however imply that it solved many open issues related with charm production, such as color octet versus singlet state. It also leaves open the very important issue of feeddown from charmonium excited states (see the following). One more open question—needed to start our simulations—is how to sample the distribution in position space. Indeed, each pQCD event generated in PYTHIA is a momentum eigenstate without any width, so by Heisenberg's

uncertainty relation they are spatially delocalized, which is unrealistic.

We proceed by assuming the form for the initial phase-space distribution to be

$$P_{\rm init}(\mathbf{r},\mathbf{p}) \propto P_{\rm PYTH}(\mathbf{p})\exp(-\mathbf{r}^2/2\sigma^2). \quad (25)$$

By setting $\sigma = 0.3$ fm we can tune the energy distribution to give a reasonable probability for the formation of the J/ψ state in pp events. However, this does not yield correct formation probabilities of χ, ψ'. This is hardly surprising, since for example the ψ' wave function has a sign change at certain distances, and the exact production amplitude is required for a projection, so an order-of-magnitude size estimate is not good enough. Since feeddown from those states contributes about 40% of the observed J/ψ, we simply refrain from any quantitative statements about pp (and very peripheral AA) collisions, focusing only on distributions *after* some amount of time spent in QGP.

C. Langevin motion of $\bar{c}c$ pairs in an expanding fireball

Finally, we model the motion of a charm quark pair in an evolving fireball. We use the same framework and programs used in Ref. [22] to examine motion of a single charm quark for propagation of an interacting pair.

We start with a large number of $\bar{c}c$ pairs produced with the PYTHIA pQCD event generation, and we randomly place them in position space throughout the fireball, using a Monte Carlo Glauber calculation.

Then, the pairs are evolved in time according to the Langevin equations

$$\frac{d\mathbf{p}}{dt} = -\eta\mathbf{p} + \boldsymbol{\xi} - \nabla U, \quad (26)$$

$$\frac{d\mathbf{r}}{dt} = \frac{\mathbf{p}}{m_c}, \quad (27)$$

where $\boldsymbol{\xi}$ corresponds to a random force and η to the drag coefficient. The condition that the Langevin equations evolve a distribution toward thermal equilibrium gives the relation $\langle\xi_i(t)\xi_j(t')\rangle = 2MT\eta\delta_{ij}\delta(t-t')$. We proceed here with our diffusion constant set by the results of Ref. [22] to be $\eta_D = \frac{2\pi T^2}{1.5M}$. and as discussed earlier with our potential as V instead of F.

Now we examine the evolution of the quark pairs as discussed before, examining pairs at mid-rapidity in a boost-invariant, two-dimensional ultrarelativistic gas simulation, the same hydrodynamical simulation used in Ref. [22]. We stop the Langevin-with-interaction evolution when $T < T_c$. The distribution over energy at different moments of the time is shown in Fig. 7.

D. Shadowing and "normal" absorption

Experimental data include not only the "QGP suppression" we study in this work but also (i) the initial-state effects (modified parton distributions in "cold nuclear matter") plus (ii) the so-called normal nuclear absorption. The way we have chosen to display PHENIX data [32] is as follows: Before we compare those with our results we "factor out" the cold

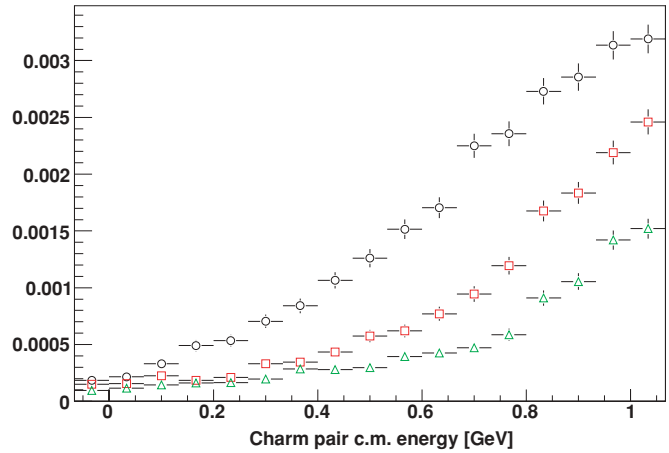

FIG. 7. (Color online) Evolving energy distribution for an ensemble of $\bar{c}c$ pairs at time moments $t = 2$, 3, and 10 fm/c (circles, squares, and triangles, respectively).

nuclear matter effects, by defining (for any given rapidity y) the following ratio of Au + Au and d + Au data,

$$R_{AA}^{\rm anomalous}(y) = \frac{R_{AA}^{\rm PHENIX}(y)}{R_{pA}(y)R_{pA}(-y)}, \quad (28)$$

to be called the "anomalous suppression." In principle these terms include only data, but unfortunately the large dAu sample taken in 2008 has not yet been analyzed (at the time of this writing), and the 2003 set has error bars that are too large. This forces us to use a model at this point, following Karsch *et al.* [33] with $R_{pA} = \exp(-\sigma_{\rm abs}\langle L\rangle n_0)$, where $\langle L\rangle$ is the mean path length of the J/ψ through nuclear matter, n_0 is the nuclear density, and $\sigma_{\rm abs}$ is the nuclear absorption cross section (parametrized from Ref. [33] to be 0.1 fm^2 for rapidity $y = 0$). Finally, for rapidity $y = 0$, we rewrite this as $[R_{pA}(y=0)]^2 = \exp(-\sigma_{\rm abs}\langle N_{\rm part}\rangle$, where $\langle N_{\rm part}\rangle$ is the density per unit area of participants in the collision plane. We further used Glauber model calculations [34] to determine $\langle N_{\rm part}\rangle$ for a given $N_{\rm part}$ at PHENIX. We divide each Au + Au data point from PHENIX by this quantity and call it $R_{AA}^{\rm anomalous}(y=0)$; these are plotted as points in Fig. 8.

E. ψ' production and feeddown

Next we calculate the ratio $N_{\psi'}/N_{J/\psi}$ in our simulations, for different centralities. There are well-known NA38/50/60 measurements of this ratio at the SPS, but at RHIC it has been measured so far only in pp collisions by the PHENIX detector [35] to be 0.14 ± 0.04, which makes the ratio of direct ψ' to J/ψ particles 0.24 as in Ref. [36]. Hopefully, the higher luminosity at RHIC will make possible a future measurement of this ratio in Au + Au collisions of various centralities.

We calculate $N_{\psi'}/N_{J/\psi}$ as follows: (i) We first run our simulation and determine the distributions $f(E)$ over the $\bar{c}c$ pair energy $E = E_{\rm CM} - 2M_c$ (in the pair center-of-mass frame). (ii) We then compare those to quasiequilibrium distributions $f_0(E)$ from simulations at fixed temperature (slightly above T_c). Since both are done for the same interaction, in the ratio $f(E)/f_0(E)$ the density of states drops out. This ratio

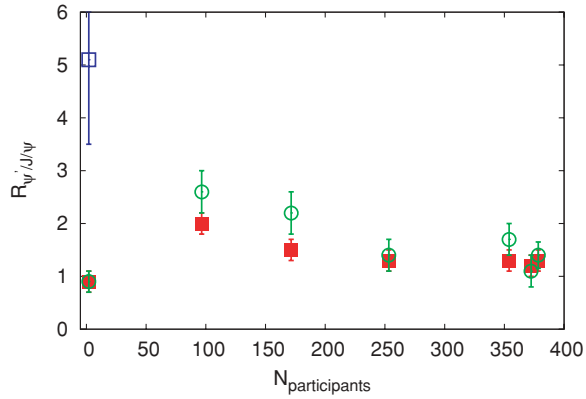

FIG. 8. (Color online) The RHIC data for R_{AA} vs $N_{\rm part}$ for J/ψ (with nuclear effects "factored out") with the results of our simulation. The open triangles (black) represent $S_{\rm bound}$ for $2\pi T D_c = 1.5$ and the potential on, the open boxes (red) represent R_{AA} for just the J/ψ with feeddown in the same simulations, the solid boxes (green) represent R_{AA} for just the J/ψ without feeddown, the open circles (blue) represent R_{AA} with $2\pi T D_c = 1.5$ and the potential off, and the solid circles (yellow) represent R_{AA} with $2\pi T D_c = 3.0$ and the potential on.

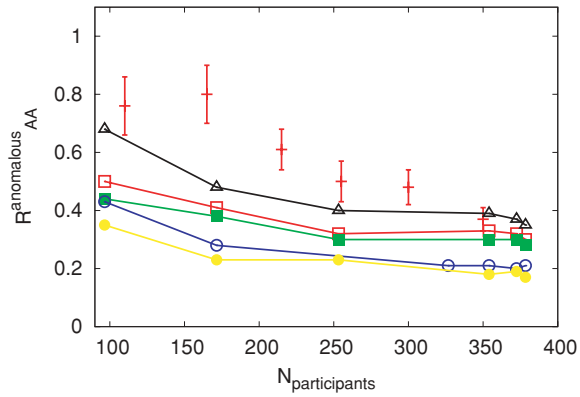

FIG. 9. (Color online) The ratio $\exp(\Delta m/T_c)N_{\psi'}/N_{J/\psi}$. The open box (blue) represents the measured ratio in pp collisions at the RHIC, the open circles (green) represent the results of our simulation for different $N_{\rm part}$ with $2\pi T D_c = 3.0$, and the solid boxes (red) represent the results of our simulation with $2\pi T D_c = 1.5$.

tells us how different the actual distribution is from that in quasiequilibrium. (iii) Then we form the *double* ratios, at two relative energies corresponding to ψ' and J/ψ masses (minus $2m_{\rm charm}$),

$$R_{\psi'/J\psi} = \frac{f(0.8\ \text{GeV})}{f_0(0.8\ \text{GeV})} \Big/ \frac{f(0.3\ \text{GeV})}{f_0(0.3\ \text{GeV})}. \tag{29}$$

This now includes nonequilibrium effects for both of them. Finally, (iv) we switch from continuum classical distributions to a quantum one, assuming that in quasiequilbrium Eq. (24) holds. If so, the particle ratio is a combination of nonequilibrium and equilibrium factors:

$$\frac{N_{\psi'}}{N_{J/\psi}} = R_{\psi'/\psi} \exp(-\Delta m/T). \tag{30}$$

The double ratio [or $\exp(\Delta M/T)N_{\psi'}/N_{J/\psi}$] is plotted versus centrality in Fig. 9 for two values of the diffusion coefficient. As one can see, it goes to unity for the most central collisions, so quasiequilibrium is actually reached in this case. We can also see that this quasiequilibrium is reached more quickly for a smaller diffusion coefficient, as it should. For mid-central bins the ψ' production is about twice as large because of the insufficient time for thermalization. This is to be compared to the experimental pp value for the ratio, which is about 5. (We remind the reader that PYTHIA plus our classical projection method does not work for pp collisions.)

Finally, we use this result to estimate the effect of feeddown from higher states. To do this, we write the final number of J/ψ particles observed as the number of directly produced J/ψ particles plus the number of J/ψ particles produced from feeddown from higher charmonium states:

$$N_{J/\psi}^{\rm final} = N_{J/\psi}^{\rm direct}\left[1 + R_{\psi'/\psi}\sum_i \left(\frac{g_i}{3}\right)\exp\left(-\frac{\Delta M_i}{T}\right)B_i\right], \tag{31}$$

where i is summed over the χ_1, χ_2, and ψ' particles that contribute significantly to feeddown, B_i represents their branching ratio into $J/\psi + \cdots$, g_i is the degeneracy of the state (divided by 3, the degeneracy of the J/ψ), and Δm_i is the mass difference between the ith state and the J/ψ. The $R_{\psi'/\psi}$ is the nonequilibrium factor; it is factored outside the sum because it is very similar for all these states.

Now we are ready to discuss the centrality dependence of the J/ψ production including the feeddown. We define for each centrality direct $N_{J/\psi}^{\rm direct}(b)$ as the total number of $c\bar{c}$ pairs in our ensemble with energy (in its rest frame) $E < 2M_{\rm charm} + 0.33$ GeV. The feedown gets its dependence on centrality from $R_{\psi'/\psi}(b)$ determined from simulation.

Finally, we determine R_{AA} as a function of the number of participants by normalizing the final yields of J/ψ with the initial yield from PYTHIA (with feeddown included) for a very peripheral collision, and we show this in Fig. 8 for various parameters for the Langevin dynamics. We also show, for the case of $2\pi T D_c = 1.5$ with the potential on, various levels of sophistication for determining R_{AA} in the same simulation: one where we simply assume $R_{AA} = S_{\rm bound}$, one where R_{AA} is determined with only direct J/ψ states, and one where proper feeddown probabilities are included. Although the results are less dramatic than what Fig. 6 would suggest, we plainly see that the predictions of our model are sensitive to the value of the diffusion coefficient, and a small diffusion coefficient with the charm and anticharm quarks in a pair interacting can help explain why the suppression observed at the RHIC is on the order of the suppression observed at SPS.

IV. INCLUDING THE "MIXED PHASE"

In our work so far, we have only examined the evolution of the $c\bar{c}$ pairs during the QGP phase, stopping the evolution wherever the fluid's temperature reached T_c. The heavy-ion collisions at RHIC seem to proceed through a "mixed phase" for central and semicentral collisions, where the medium spends a significant amount of time near T_c, as described in Ref. [37]. For our determination of R_{AA} versus $N_{\rm part}$, the

mixed phase is insignificant: The percentage of J/ψ particles does not change significantly after the initial time as Fig. 6 suggests. Since we do not pretend to know the dynamics of charmonium in the mixed phase, we are satisfied that even the extreme limit of unchanged Langevin evolution through the mixed phase does not significantly change our results in Fig. 8. However, for describing the development of momentum anisotropy of charmonium in a semicentral collision [$v_2(p_t)$], the mixed phase is of great importance and we are forced to model it for a typical collision in the minimum-bias data set.

In various hydrodynamic models that describe heavy-ion collisions, the region of roughly $T = (0.9\text{–}1.1)T_c$ is treated as a separate "mixed phase" distinct from QGP and hadronic phases. Indeed, it has a very different equation of state: Whereas the temperature and pressure remain nearly constant, the energy and entropy densities jump by a large factor.[4]

What is very important for the present paper is that the near-T_c region occupies a significant fraction of the fireball evolution, in spite of being a very narrow interval in terms of T. Indeed, one should rather focus not on T but on the entropy density s, which shows a simple monotonic decrease with time $s \sim 1/\tau$ for all three phases.

For a quantitative description of the mixed phase we used hydrodynamical calculations, known to describe radial and elliptic flow well, such as the work by Teaney *et al.* [37]. It follows from their solution that the "mixed phase" persists for about 5 fm/c after the deconfined phase, which is comparable to the lifetime of the deconfined phase at the very center of the fireball. Thus it is by no means a small effect and should be included in any realistic treatment of a heavy-ion collision.

The flow during this time was found to be well approximated by a Hubble-like expansion with radial velocity $v = Hr$ and time-independent $H \approx 0.075$ fm^{-1} for central collisions. Then, the anisotropy of this expansion can be parameterized similarly:

$$v_i = H_i x_i, \tag{32}$$

with $i = 1, 2$ and where $H_x = 0.078$ fm^{-1} and $H_y = 0.058$ fm^{-1}; thus anisotropy is only about 80% by this late stage. In the following we will consider collisions with a nonzero impact parameter of $b = 6.5$ fm. It is fair to say that we have a fairly reasonable understanding of how the medium flows for these later stages. Thus in our simulations we have used those parametrizations instead of numerical solutions to hydrodynamics, which were necessary for the QGP phase.

Let us start with two extreme scenarios for the dynamics of the charm quarks during this phase of the collision:

(i) The charm quarks are completely "stopped" in the medium, so that they experience the same Hubble-like flow as matter.

(ii) $\bar{c}c$ pairs do not interact at all with the medium near T_c, moving ballistically with constant velocity for the corresponding time in the collision.

If the first scenario were true, the effect of Hubble flow would be to increase all momenta of particles by the same multiplicative factors $p_i(t) = p_i(0)\exp(H_i t)$. With sufficiently high drag, Langevin dynamics would bring the charm quarks rapidly to a thermal distribution, and since $M \gg T$ it is a good approximation in this case to say that the heavy quarks have been "stopped." However, we will show in the following that at the "realistic" value used for the drag η_c this does not happen during the time allocated to the mixed phase; there is instead ongoing "stopping" of the charm quarks relative to fluid elements. [This also will be important for the evolution of the azimuthal anisotropy $v_2(p_t)$ for single charm and for charmonium.] The second scenario predicts $v_2(p_t)$ for single charm quarks that is far smaller than what is measured. We do not consider this scenario further even though something might be said for modeling charmonium in the mixed phase as interacting far less than single charm.

Several single charm p_t distributions are shown in Fig. 10 (normalized for simplicity to unity). The initial distribution after hard production predicted by PYTHIA is the largest at high p_t. This is compared to the Langevin evolution before (squares) and after (triangles) the mixed phase, for a semicentral RHIC collision ($b = 7$ fm). To see that radial flow still is important, we have also show what happens if Langevin evolution happens on top of unmoving fixed-T plasma (circles). This comparison demonstrates once again the main point of this paper, that for charm quarks and charmonium in a heavy-ion collision equilibration is never complete, even in momentum space, so the specific time scales of different phases of matter are of fundamental importance.

Unfortunately, in the near-T_c region it is much less clear how to describe the c-$\bar{c}$ interaction. As we have learned from lattice

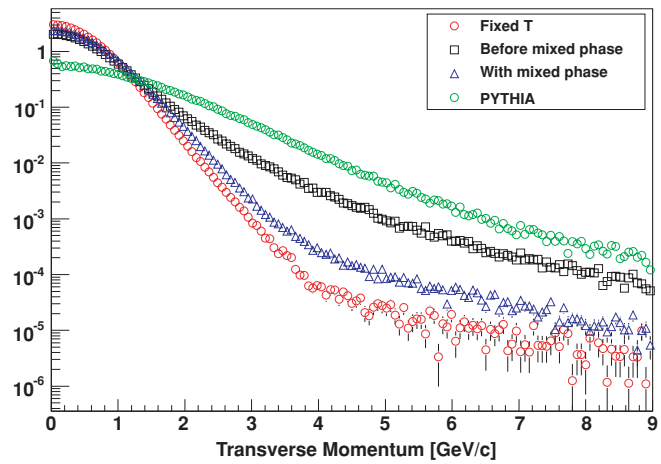

FIG. 10. (Color online) The charm p_t distribution after the mixed phase compared with the distribution without flow, the distribution originating from PYTHIA, and the distribution before the mixed phase.

[4]Although the exact nature of matter in the near-T_c region is not yet understood, let us mention that the original "mixed phase" description, originating from the notion of the first-order phase transition, cannot be true, as "supercooling" and bubble formation expected in this case are not observed experimentally. Lattice gauge theory suggests a smooth crossover-type transition, with a high but finite peak in the specific heat. Recently, there has been renewed interest in this region, after the so-called magnetic scenario for it was proposed [38,39], describing it as a plasma containing a significant fraction of magnetic monopoles.

data, the difference between free-energy and potential-energy potentials is very drastic in this case: In the former case the tension (the force from the linear potential) disappears whereas in the latter it becomes about five times stronger than it is in vacuum. As discussed in Refs. [40,41], the latter is presumably due to a metastable electric flux tube.

Which potential to use depends on the time scales of the c-$\bar{c}$ dynamics, which are not well understood at this point. Therefore we took for now a conservative approach, assuming that at the near-T_c stage charm pairs interact according to the simple Coulomb interaction $V = -\alpha_s/r$. Additionally, in our model for this phase we assume the interaction of the charm quarks with the medium can be modeled with the same Langevin dynamics with the temperature approximated as a fixed $T = T_c$ and the flow as previously given. We found that with the simple Coulomb potential used in the mixed phase, the survival probability dropped slightly but not significantly, and although we do not discuss other possibilities in this work further, in principle this can be changed if the potential to be used has significant tension.

One final interesting observable would be a measurement of charmonium elliptic flow, characterized by the azimuthal anisotropy parameter $v_2 = \langle \cos(2\phi) \rangle$, induced by ellipticity of the flow on charmed quarks. A measurement with low statistics has been already made at PHENIX [42]. At both PHENIX and STAR higher statistics data on tape are now being worked on. The result of our calculation of $v_2(p_t)$, both for single charm quarks and for the J/ψ, is shown in Fig. 11.

Greco, Ko, and Rapp also made predictions for the v_2 for J/ψ [43], with a model where all of the final J/ψ states coalesced from the single charm quark "thermal+flow" distribution one would get from a typical minimum-bias RHIC collision. We have in common the strong interaction of charm with the medium and the coalescence from these charm quarks of the observed J/ψ particles. As it turns out, our predictions are similar: the value of v_2 of J/ψ should be less than the value of v_2 of single charm for low p_t, but then increase past the v_2 value of single charm at $p_t > 3$ GeV.

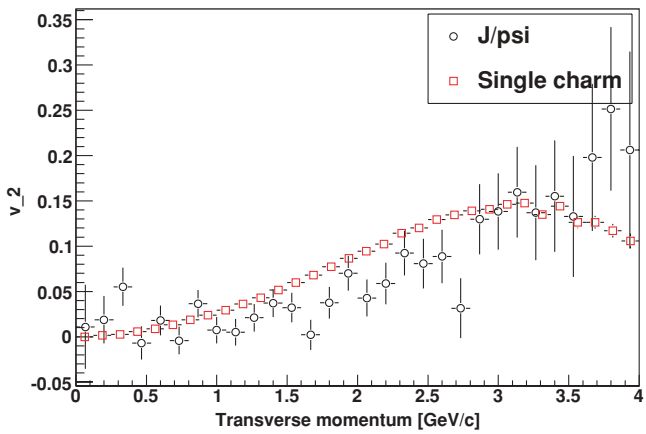

FIG. 11. (Color online) The azimuthal anisotropy vs transverse momentum for single charm and for J/ψ.

V. SUMMARY

We have studied a relaxation process of a $\bar{c}c$ pair produced by hard processes in heavy-ion collision throughout the sQGP stage using hydrodynamics plus Langevin dynamics. The main elements of the paper are (i) inclusion of the interaction force between charm quarks and (ii) emphasis on deviations from equilibrium during the finite QGP lifetime.

Our main finding is that the lifetime of sQGP is not sufficient to reach the equilibrium distribution of the pairs in space, allowing for a significant fraction of $J/\psi \sim 1/2$ to survive. This probability for charmonium dissociation in sQGP is larger than in earlier perturbative estimates, or for Langevin diffusion ignoring mutual interaction.

That is why there is no large difference between suppression at RHIC and SPS, in spite of the longer QGP lifetime in the former case. Although the momentum relaxation is rather rapid, we found that later evolution reaches the so-called quasiequilibrium regime, which is maintained throughout QGP expansion. The spatial distributions after some time develop a "core" in which $\bar{c}c$ pairs remain in close proximity owing to the remaining effective attraction in sQGP, combined with a relatively slow leakage into a spreading tail toward large r. We propose quasiequilibrium as the clue to an explanation of the apparently thermal ratios of ψ' and J/ψ, especially at SPS.

The shape of the centrality dependence of our survival probability is in agreement with data. Therefore, although we have not yet directly evaluated "nondiagonal" recombination, we think that most of the J/ψ particles observed at SPS and RHIC are still from the "diagonal" pairs. This and other issues will of course be clarified, as more simulations and data in different kinematic domains become available.

The calculation is extended to the near-T_c region—known as a "mixed phase" in hydrodynamical calculations. Its duration for RHIC collisions is about 5 fm/c, which is comparable to that of the QGP. We have used a simple Hubble-like parametrization and a minimal Coulomb potential, predicting both the charmonium p_t spectra and azimuthal asymmetry parameter v_2 that is expected to be measured soon.

ACKNOWLEDGMENTS

We thank P. Petreczky for providing lattice data on the internal energy $V(T, r)$ used in this work. C. Young would like to thank K. Dusling for useful discussions on various topics in this work. We especially thank D. Teaney for permitting us use of his hydrodynamics+Langevin code and providing much needed assistance. This work is partially supported by the US Department of Energy Grant Nos. DE-FG02-88ER40388 and DE-FG03-97ER4014.

APPENDIX A: CLASSICAL VERSUS QUANTUM DYNAMICS

In this paper, we take phase-space distributions of $\bar{c}c$ pairs and evolve them according to the Fokker-Planck/Langevin equations, which describe the nonequilibrium evolution of

phase-space distributions during the QGP era. After the evolution is finished and the medium returns to the hadronic phase, our classical distribution $f(\mathbf{x}, \mathbf{p}, t)$ has to be projected into charmonium quantum states.

He we examine how classical and quantum dynamics correspond to each other in equilibrium, when both are easily available. We simplify by examining the thermal distributions for a Coulombic system, with $V \sim 1/r$. One can calculate the density of states for the classical system:

$$\begin{aligned} Z &= \int dr dp (4\pi)^2 r^2 p^2 \exp[-(p^2/2\mu - e^2/r)/T] \\ &= \int dE \int dr dp (4\pi)^2 r^2 p^2 \\ &\quad \times \exp(-E/T)\delta(E - p^2/2\mu + 1/r) \\ &= \int dE \exp(-E/T) \int_{\max(0,\sqrt{2\mu E})}^{\infty} dp \frac{e^2 p^2}{(p^2/2\mu - E)^4}. \end{aligned}$$

As one can see, this integral is divergent for $E > 0$. This means that this distribution is not normalizable and in thermal equilibrium all pairs are ionized. For $E < 0$, we see from examining the partition function that

$$\rho(E) \propto (-E)^{-5/2}. \tag{A1}$$

Now we calculate the quantum mechanical density of states for $E < 0$,

$$\rho(E) = \Sigma_{n=1}^{\infty} n^2 \delta\left(E + \frac{C}{n^2}\right), \tag{A2}$$

which can be approximated by considering an integral:

$$\begin{aligned} \int_{-\infty}^{E} dE' \rho(E') &= \Sigma_{i=1}^{\infty} i^2 \theta\left(E + \frac{C}{i^2}\right) \\ &\sim E^{-3/2} \text{ for large enough } E. \end{aligned}$$

Thus, $\rho(E) \sim E^{-5/2}$ for E close to zero. Therefore for highly excited states the correspondence principle holds and the classical thermal distribution is recovered. However, the classical density of states is not as good of an approximation as the quantum-mechanical density of states for the lowest bound state.

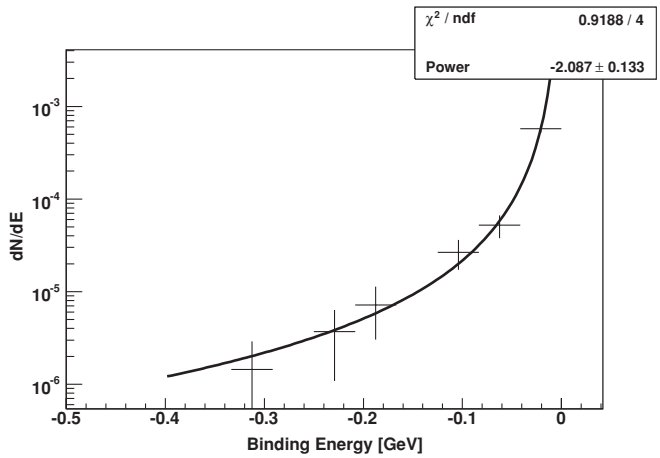

FIG. 12. The points show the density of states for an ensemble of $\bar{c}c$ pairs at a fixed temperature $T = 1.5T_c$ obtained by long-time Langevin evolution, compared to a fit with power 2.1 (curve), close to classical nonrelativistic thermal distribution.

We also tested whether Langevin simulations lead to the correct classical density of states, after some relaxation time. The result of evolving an ensemble of $\bar{c}c$ pairs at a fixed temperature according to classical Langevin dynamics shown in Fig. 12 shows that equilibrium is indeed obtained.

APPENDIX B: COALESCENCE PROBABILITY

After all distributions at the end of the QGP era are determined, the next step is to calculate the probabilities of it materializing as a particular charmonium state.

One approach is based on the Wigner probability distribution. For any wave function $\psi(\mathbf{r})$,

$$W_{\psi}(\mathbf{r}, \mathbf{p}) = \frac{1}{\pi^3} \int d^3 y \psi^*\left(\mathbf{r} + \frac{\mathbf{y}}{2}\right) \psi\left(\mathbf{r} - \frac{\mathbf{y}}{2}\right) e^{i\mathbf{p}\cdot\mathbf{y}}. \tag{B1}$$

The wave function for J/ψ was easily calculated numerically and then fitted to a Gaussian $\psi_i(x) \propto e^{-3.8r^2/\text{fm}^2}$. This leads immediately to the following parametrization of the J/ψ's Wigner distributions (where the constant is in fm^{-2}):

$$W_{J/\psi}(x, p) = \frac{1}{\pi^3} \exp(-7.6r^2 - p^2/7.6). \tag{B2}$$

Many properties for the Wigner transform so defined may be discussed but for our purposes here we should note that

$$\int W_{\psi}(x, p) dp = |\psi(x)|^2 \tag{B3}$$

and for another wave function $\chi(x)$'s Wigner transform $W_{\chi}(x, p)$ we have

$$\int W_{\psi}(x, p) W_{\chi}(x, p) dx dy = \tfrac{1}{(2\pi)^3} |\langle\psi|\chi\rangle|^2, \tag{B4}$$

because this is what we need to properly normalize our distributions and to compute overlaps.

So, for our phase-space distribution at any given time $f(\mathbf{x}, \mathbf{p}, \tau)$, we model our probability of a pair being measured in the J/ψ state as

$$P_{J/\psi}(\tau) = (2\pi)^3 \int f(\mathbf{r}, \mathbf{p}, \tau) W_{J/\psi}(\mathbf{r}, \mathbf{p}) d^3x d^3p. \tag{B5}$$

We project the pairs onto the J/ψ state not only at the onset of the calculation but also throughout the time evolution, monitoring in this way the probability of J/ψ production. We use this approach to estimate the coalescence probability for the distribution in Sec. II.

Later on we switched to the "energy projection method," which is ultimately used for projection into χ, ψ' states as well as into J/ψ. It is based on the distribution over $\bar{c}c$ energy, in the pair rest frame, calculated with the (zero-temperature) Cornell potential. One projection, used in Fig. 8, is to all bound states, defined by

$$E_{\text{CM}} = V_{\text{Cornell}}(r) + \frac{p_{\text{rel}}^2}{M_c} < 0.88 \text{ GeV}. \tag{B6}$$

Later on, we differentiate between various charmonium states again by examining the $\bar{c}c$ pair's energy in its rest frame, and comparing it with the energies of solutions to Schrödinger's equation using the Cornell potential. For example, the lowest s-state solution, using the charm quark mass, has energy $E = 0.33$ GeV; therefore we count all $\bar{c}c$ pairs in our simulation with energy below 0.33 GeV as existing in the J/ψ state.

[1] E. V. Shuryak, Phys. Lett. **B78**, 150 (1978); Yad. Fiz. **28**, 796 (1978); Phys. Rep. **61**, 71 (1980).
[2] D. Kharzeev and H. Satz, Phys. Lett. **B334**, 155 (1994).
[3] A. Andronic, P. Braun-Munzinger, K. Redlich, and J. Stachel, Phys. Lett. **B571**, 36 (2003).
[4] T. Matsui and H. Satz, Phys. Lett. **B178**, 416 (1986).
[5] F. Karsch, M. T. Mehr, and H. Satz, Z. Phys. C **37**, 617 (1988).
[6] S. Datta, F. Karsch, P. Petreczky, and I. Wetzorke, arXiv:hep-lat/0208012; M. Asakawa and T. Hatsuda, Nucl. Phys. **A715**, 863c (2003).
[7] A. Mocsy, P. Petreczky, and J. Casalderrey-Solana, Nucl. Phys. **A783**, 485 (2007).
[8] A. Mocsy and P. Petreczky, PoS **LAT2007**, 216 (2007).
[9] L. Grandchamp and R. Rapp, Nucl. Phys. **A715**, 545 (2003).
[10] E. V. Shuryak and I. Zahed, Phys. Rev. D **70**, 054507 (2004).
[11] C.-Y. Wong, Phys. Rev. C **72**, 034906 (2005); W. M. Alberico, A. Beraudo, A. De Pace, and A. Molinari, Phys. Rev. D **72**, 114011 (2005).
[12] Q. J. Ejaz, T. Faulkner, H. Liu, K. Rajagopal, and U. A. Wiedemann, J. High Energy Phys. 04 (2008) 089.
[13] F. Karsch and R. Petronzio, Phys. Lett. **B193**, 105 (1987).
[14] R. L. Thews, Nucl. Phys. **A783**, 301 (2007); R. Rapp, Eur. Phys. J. C **43**, 91 (2005).
[15] F. Karsch, D. Kharzeev, and H. Satz, Phys. Lett. **B637**, 75 (2006).
[16] G. Aarts, C. Allton, M. B. Oktay, M. Peardon, and J. I. Skullerud, Phys. Rev. D **76**, 094513 (2007).
[17] O. Kaczmarek and F. Zantow, PoS **LAT2005**, 192 (2006).
[18] K. Dusling and C. Young, arXiv:0707.2068 [nucl-th].
[19] O. Kaczmarek, S. Ejiri, F. Karsch, E. Laermann, and F. Zantow, Prog. Theor. Phys. Suppl. **153**, 287 (2004).
[20] E. V. Shuryak, Phys. Rev. C **55**, 961 (1997); arXiv:nucl-th/9605011.
[21] S. S. Adler *et al.* (PHENIX Collaboration), Phys. Rev. Lett. **94**, 082301 (2005).
[22] G. D. Moore and D. Teaney, Phys. Rev. C **71**, 064904 (2005).
[23] J. M. Maldacena, Adv. Theor. Math. Phys. **2**, 231 (1998) [Int. J. Theor. Phys. **38**, 1113 (1999)].
[24] J. Casalderrey-Solana and D. Teaney, Phys. Rev. D **74**, 085012 (2006).
[25] C. P. Herzog, A. Karch, P. Kovtun, C. Kozcaz, and L. G. Yaffe, J. High Energy Phys. 07 (2006) 013; S. S. Gubser, arXiv:hep-th/0605182; A. Buchel, arXiv:hep-th/0605178; S.-J. Sin and I. Zahed, arXiv:hep-ph/0606049.
[26] B. A. Gelman, E. V. Shuryak, and I. Zahed, Phys. Rev. C **74**, 044909 (2006); **74**, 044908 (2006).
[27] J. Liao and E. Shuryak, Phys. Rev. C **75**, 054907 (2007).
[28] S. S. Adler *et al.* (PHENIX Collaboration), Phys. Rev. Lett. **96**, 012304 (2006).
[29] X. Dong, AIP Conf. Proc. **828**, 24 (2006) [Nucl. Phys. **A774**, 343 (2006)].
[30] H. Sorge, E. V. Shuryak, and I. Zahed, Phys. Rev. Lett. **79**, 2775 (1997).
[31] T. Sjöstrand, S. Mrenna, and P. Skands, J. High Energy Phys. 05 (2006) 026.
[32] A. Adare *et al.* (PHENIX Collaboration), Phys. Rev. Lett. **98**, 232301 (2007).
[33] F. Karsch, D. Kharzeev, and H. Satz, Phys. Lett. **B637**, 75 (2006).
[34] D. Kharzeev and M. Nardi, Phys. Lett. **B507**, 121 (2001).
[35] A. Adare *et al.* (PHENIX Collaboration), Phys. Lett. **B670**, 313 (2009).
[36] S. Digal, P. Petreczky, and H. Satz, Phys. Rev. D **64**, 094015 (2001).
[37] D. Teaney, J. Lauret, and E. V. Shuryak, arXiv:nucl-th/0110037.
[38] J. Liao and E. Shuryak, Phys. Rev. C **75**, 054907 (2007).
[39] M. N. Chernodub and V. I. Zakharov, Phys. Rev. Lett. **98**, 082002 (2007).
[40] J. Liao and E. Shuryak, Phys. Rev. C **77**, 064905 (2008).
[41] J. Liao and E. Shuryak, arXiv:0804.4890 [hep-ph].
[42] C. Silvestre (PHENIX Collaboration), arXiv:0808.2925 [nucl-ex].
[43] V. Greco, C. M. Ko, and R. Rapp, Phys. Lett. **B595**, 202 (2004).